Available online at www.sciencedirect.com

SCIENCE DIRECT

Experimental Cell Research 306 (2005) 142 – 149

Experimental Cell Research

www.elsevier.com/locate/yexcr

Possible role of deep tubular invaginations of the plasma membrane in MHC-I trafficking

Ramiro H. Massol, Jakob E. Larsen, Tomas Kirchhausen*

Department of Cell Biology and The CBR Institute for Biomedical Research, Harvard Medical School, 200 Longwood Avenue, Boston, MA 02115, USA

Received 2 December 2004, revised version received 18 January 2005
Available online 23 March 2005

Abstract

Tubules and vesicles are membrane carriers involved in traffic along the endocytic and secretory routes. The small GTPase Arf6 regulates a recycling branch of short dynamic tubular intermediates used by major histocompatibility class I (MHC-I) molecules to traffic through vesicles between endosomes and the plasma membrane. We observed that Arf6 also affects a second network of very long and stable tubules containing MHC-I, many of which correspond to deep invaginations of the plasma membrane. Treatment with wortmannin, an inhibitor of phosphatidylinositol-3-phosphate kinase, prevents formation of the short dynamic tubules while increasing the number of the long and very stable ones. Expression of NefAAAA, a mutant form of HIV Nef, increases the number of cells containing the stable tubules, and is used here as a tool to facilitate their study. Photoactivation of NefAAAA-PA-GFP demonstrates that this molecule traffics from endosomes to the tubules. Finally, live-cell imaging also shows internalization of MHC-I molecules into these tubules, suggesting that this is an additional route for MHC-I traffic.

Keywords: MHC-I; Tubules; NefAAAA; Trafficking; Nef; Endocytosis

Introduction

Most intracellular trafficking carriers are relatively small vesicles that pinch-off from the source membrane compartment carrying cargo to their final cellular destinations. Nonetheless, several imaging approaches have provided evidence that tubular structures are also important carriers for directed membrane traffic. For instance, images showing the movement of VSVG and GPI-anchored proteins fused with fluorescent proteins demonstrated the existence of an exocytic tubular-based pathway emanating from the trans-Golgi network and reaching the plasma membrane [1–5]. Similarly, live-cell imaging demonstrated the existence of a polarized route of transport for MHC class II molecules mediated by tubules that emanated from the loading endosomal compartment and stretched toward the immune synapse in activated dendritic cells [6]. Static views obtained by electron or fluorescence microscopy showed presence of tubules within the endosomal compartment, perhaps also involved in intra-endosomal traffic [7]. Finally, deep tubular invaginations from the plasma membrane are found in different cell types and are proposed to participate in specialized forms of traffic such as recycling of synaptic vesicles (see review in [8]), transcytosis in polarized epithelial cells [9,10] and uptake of cholera toxin [11].

One class of molecules present in tubular structures is the major histocompatibility class I (MHC-I) proteins, which display endogenous and antigenic peptides on the cell surface for surveillance by T $CD8^+$ lymphocytes. These molecules constantly cycle between the surface and the cell interior in a poorly understood process. MHC-I lacks sorting signals recognized for endocytosis via clathrin-coated vesicles [12], and the identity of the endocytic carriers for MHC-I is currently unknown. On the other hand, it has been shown that MHC-I recycles from endosomes to the cell surface through tubules modulated by Arf6, EHD1, Rab22, and Rabenosyn-5 [13–16].

* Corresponding author. Fax: +1 617 278 3131.
E-mail address: kirchhausen@crystal.harvard.edu (T. Kirchhausen).

0014-4827/$ - see front matter © 2005 Elsevier Inc. All rights reserved.
doi:10.1016/j.yexcr.2005.01.021

In the course of previous studies of MHC-I traffic and its perturbations by expression of Nef, a human immunodeficiency virus encoded protein that increases the internalization and degradation of MHC-I molecules, we observed long and relatively stable tubes containing MHC-I radiating from a perinuclear endosomal compartment towards the cell surface [17]. Although these tubules were also observed in cells not expressing Nef, the number of cells exhibiting these structures increased dramatically upon expression of the Nef mutant NefAAAA, which cannot interact with the endosomal sorting protein PACS-1. Hence, here, we use expression of NefAAAA as a tool to study this tubular compartment. We find that these tubules contain NefAAAA and represent deep invaginations of the plasma membrane that remain open to the cell exterior. Live-cell imaging shows that MHC-I molecules can move from the cell surface to endosomes along these tubules, whereas transferrin receptor is mostly excluded. We propose that these tubules might constitute an additional route for MHC-I traffic.

Results and discussion

PI3K affects the appearance of the NefAAAA/MHC-I membrane tubular network

Expression in U373mg astrocytoma cells of the membrane-bound Nef mutant NefAAAA results in a substantial increase (~3- to 5-fold) in the number of transduced cells displaying a branched membrane tubular network containing NefAAAA (Figs. 1A and B and [17]). This phenotype is

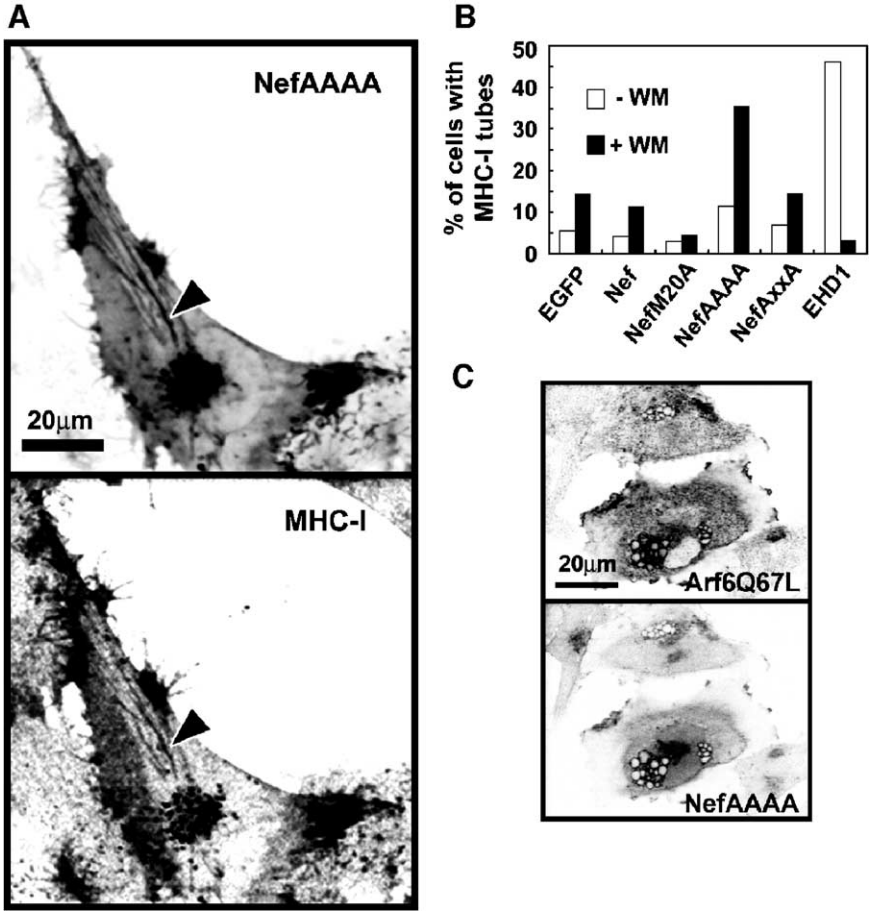

Fig. 1. NefAAAA and MHC-I membrane tubular network. (A) Expression of NefAAAA-EGFP (by transduction) in astrocytoma U373mg cells [17] results in the appearance of a large number of long tubules containing NefAAAA and MHC-I. Representative images are displayed using an inverted monochrome scale to facilitate visualization. The same results were observed in more than 100 cells from 6 different experiments. (B) Inhibition of PI3-K by treatment with 0.2 μM wortmannin (WM, black bars) for 30 min results in an increase in the fraction of astrocytoma U373mg cells exhibiting the long tubules containing MHC-I. In contrast, the same treatment in HeLa cells and astrocytes (not shown) expressing EGFP-EHD1 results in a significant decrease in the number of cells exhibiting the EHD1-labeled Arf6-recycling tubules. MHC-I labeling was done by incubation of the live cells for an additional 30 min with Alexa594-labeled antibodies specific for the ectodomain of MHC-I followed by fixation and epifluorescence microscopy imaging. For each condition, between 200 and 300 cells were scored from a total of 3 experiments. (C) Co-expression of NefAAAA (by transduction) with HA-tagged Arf6Q67L (by transfection), a constitutive active mutant form of Arf6 locked in the GTP-state, prevents the formation of the tubular network. Similar results (not shown) were obtained by expression of wild type Arf6 or Arf6T27N, a constitutively inactive mutant form of Arf6 locked in the GDP-state. Cells were transduced and then transfected 3 days later. Two days after transfection, cells were fixed and imaged. Representative images correspond to data obtained from more than 100 cells co-expressing NefAAAA with Arf6 wild type or mutants from 3 independent experiments.

maintained in cells for weeks without a change in the number of cells containing tubules, suggesting that their appearance is not harmful to the cells. Moreover, long-term expression of NefAAAA did not induce apoptosis or cell death. The tubules containing NefAAAA and MHC class I are very long (Fig. 1A), and those spanning all the way from the plasma membrane to the endosomal compartment did not change their shape significantly for at least the duration of the time-lapse imaging experiments, typically 10 min (Supplementary Movie 1 in Appendix A). Similar results were obtained using HeLa and Jurkat T cells, although the number of cells showing the phenotype was smaller. In addition to MHC-I, the tubules contain β1-integrin and EHD1 molecules [17], indicating that these structures might be related to the Arf6-tubular recycling system previously described in the absence of Nef [16,18]. Transferrin receptors, as well as clathrin, are significantly excluded from these tubules (Supplementary Fig. 1s in Appendix A), suggesting that these structures have a distinct membrane composition compared to the bulk of the plasma membrane. Nevertheless, the surface density of MHC-I on the plasma membrane and in the tubules is similar, indicating that there is no active sorting of MHC-I into these structures. Appearance of the tubular network is dramatically increased by expression of a form of Nef hindered in its ability to interact with PACS-1, since expression of wild type Nef, or two other mutants (NefM20A or NefAxxA) used as controls, capable of interacting with PACS-1 does not increase the number of cells showing this phenotype (Fig. 1B). A similar tubular phenotype was observed in U373mg cells only expressing the MHC-I molecule HLA-A2 fused to EGFP, indicating that this network does not originate from crosslinking MHC-I with antibodies used for the uptake experiments (Supplementary Movie 2 in Appendix A). The relatively low frequency (<20%) of cells exhibiting the expanded tubular network elicited by expression of NefAAAA suggests that its existence is regulated.

Generation of the large tubules is prevented by overexpression of Arf6Q67L, the dominant active mutant form of Arf6 (Fig. 1C), or of wild type Arf6 or the mutants, Arf6T27N and Arf6T157A (not shown) indicating that perturbations in the function of Arf6-regulated pathways also affect the NefAAAA-induced tubules. We believe that the tubular network generated by Nef expression differs, however, from the MHC-I-recycling tubules regulated by Arf6. For example, transient inhibition of phosphatidylinositol-3-phosphate kinase (PI3-K), which activates ARNO [19,20], a GEF for Arf6 [21], leads to a dramatic increase in the number of cells exhibiting tubules regardless of whether Nef is expressed or not (Fig. 1B), whereas the same treatment results in a significant decrease in the number of HeLa cells showing the Arf6-recycling tubules induced by overexpression of EHD1 (Fig. 1B). Although transient expression of EHD1 in U373mg cells also results in the appearance of the Arf6-recycling tubules, less than 5% of the cells displayed this phenotype; this is not due to a decrease in transfection efficiency or expression level, however (not shown). Nevertheless, like with HeLa cells, treatment of U373mg astrocytes with wortmannin also decreased the number of tubules generated by expression of EHD1 (not shown). We confirmed previous observations [22–24] showing that cell viability and net uptake of transferrin are not affected by wortmannin treatment (not shown). In addition, a similar inhibition of PI3-K prevents transport of MHC-I from Arf6-early endosomes to the Arf6-recycling tubules in HeLa cells [25].

Movement of NefAAAA in the tubulo-vesicular network

As a way to distinguish whether the NefAAAA-induced tubules consist of a linear array of closely associated vesicles or tubular structures, we studied the movement of NefAAAA-EGFP molecules within the tubular network. Fluorescence recovery after photobleaching of NefAAAA-EGFP, performed in cells displaying the tubular phenotype, showed movement of non-photobleached NefAAAA molecules from opposite ends towards the center of the bleached region of the tubule (Fig. 2A). There is some variability but no clear tendency in the recovery rate for molecules entering the photobleached region of the tubules from either side. Nevertheless, the recovery rate is fast (~0.4 μm/s, ±0.1 μm/s) and corresponds to a one-dimensional diffusion coefficient of 0.39 ± 0.07 $\mu m^2/s$, a value characteristic of free lateral diffusion of membrane-bound proteins [26]. Noticeably, the recovery of the fluorescent signal was gradual and did not involve movement of punctuate structures suggesting that vesicular carriers are not involved in the recovery (Fig. 2A). This study was complemented by following the behavior of photoactivated NefAAAA (fused to a photoactivatable GFP (PA-GFP) [27]. We found a bi-directional movement of NefAAAA-PA-GFP from the site of photoactivation, with a similar diffusion rate as in the case of photobleaching, and the absence of moving fluorescent vesicles moving along the tubular tracks emanating from this region (Supplementary Movie 3 in Appendix A). Similarly, we also observe that the tubules can receive NefAAAA molecules residing in the endosomal compartment since photoconversion of NefAAAA-PA-GFP molecules located in the perinuclear endosomes led to the fast appearance of fluorescent molecules in the adjacent tubules (Fig. 2B).

Movement of MHC-I molecules into the tubular network

Considering that the ends of many of the NefAAAA-labeled tubules are in close proximity with the plasma membrane, we investigated whether the tubules could receive traffic of MHC-I molecules from the plasma membrane. Indeed, upon addition to the medium of fluorescent antibodies specific for the ectodomain of MHC-I molecules, we observed decoration of the plasma membrane followed by rapid filling (within 1 min) of the

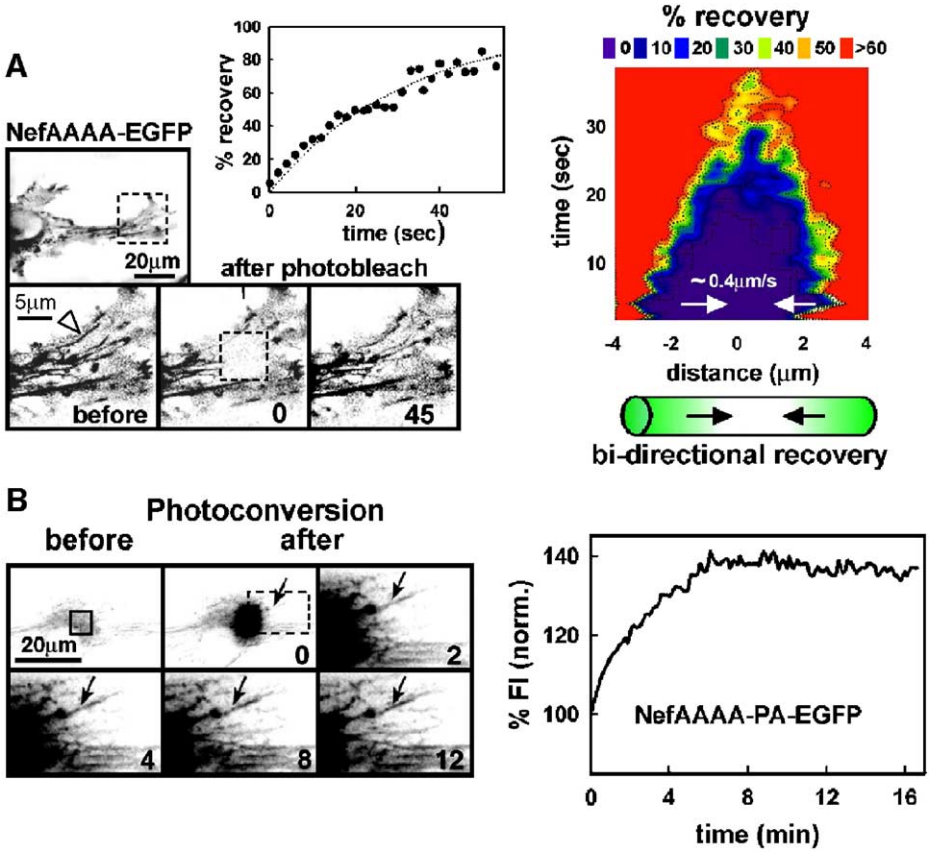

Fig. 2. Movement of membrane-bound NefAAAA along the membrane tubular network. (A) U373mg astrocytoma cells expressing NefAAAA-EGFP were photobleached in a region containing membrane tubules (stippled box) and the rate of fluorescence recovery was determined in selected photobleached tubules and snapshots as a function of time (seconds) are shown. The plot shows the fluorescence recovery after photobleaching as a function of time for the selected tubule (arrow head). Color plot shows a kymograph representation of the fluorescence recovery after photobleaching corresponding to the same tubule. The tubule was first segmented and linearized using Slidebook and Image J, followed by pseudocolor display of fluorescence relative intensities along the tubule as a function of time. Data are representative of 6 different photobleaching experiments from two different transductions. (B) U373mg astrocytoma cells expressing NefAAAA-PA-GFP were identified by their weak fluorescent signal and NefAAAA-PA-GFP was photoactivated in a region containing membrane tubules (box). The images presented as a function of time (min) correspond to a region of the cell (stipple box) and illustrate the kinetics of NefAAAA-PA-GFP traffic after photoactivation. The plot shows the increase in fluorescence as a function of time for a selected tubule (arrow). Data are representative of 4 different photoactivation experiments from two different transductions.

tubules starting from the end proximal to the cell surface (Fig. 3A, arrowheads, stippled circle regions and plot). This fluorescent signal does not represent unbound antibody captured within the tubules as part of the fluid phase since its signal is much higher than the signal in the medium, and over time it reaches a similar value as the cell surface bound antibodies.

In view of the close proximity of the tubules to the cell surface and the fast entry of MHC-I antibodies into these structures, we considered the possibility that some of the tubules are opened to the cell surface. Results from three different experiments support this view. First, we labeled the NefAAAA-tubular network with the fluorescent antibody specific for MHC-I. Cells were then transferred to 4°C and subjected to 4 consecutive washes with acid buffer within a total period of 1 min. This procedure results in the substantial removal of the antibodies from the plasma membrane and from the NefAAAA-containing tubules, but not from the perinuclear endosomes. It is known that MHC-I molecules contained in the recycling-tubular compartment regulated by Arf6 are resistant to acid wash treatments [18], a result that is consistent with our view that the tubules induced by Nef are distinct than those regulated by Arf6.

The second evidence supporting a direct connection between the tubules and the plasma membrane was obtained by establishing their accessibility to an antibody present in the medium surrounding fixed NefAAAA cells under non-permeabilizing conditions. In this case, cells were incubated with the anti-MHC-I antibodies, fixed and, in the absence of detergent, further incubated with HRP-tagged antibodies specific for the anti-MHC-I antibodies. Presence of the HRP–antibody complexes was determined by DAB staining and its location established by electron microscopy. Fig. 3C shows examples of tubules (or their sections) stained with the electron-dense DAB. Fig. 3D shows control for unspecific staining performed in cells expressing Nefwt, which exhibit a strong reduction in total levels of MHC-I. Since the HRP-tagged antibody specific for the antibodies

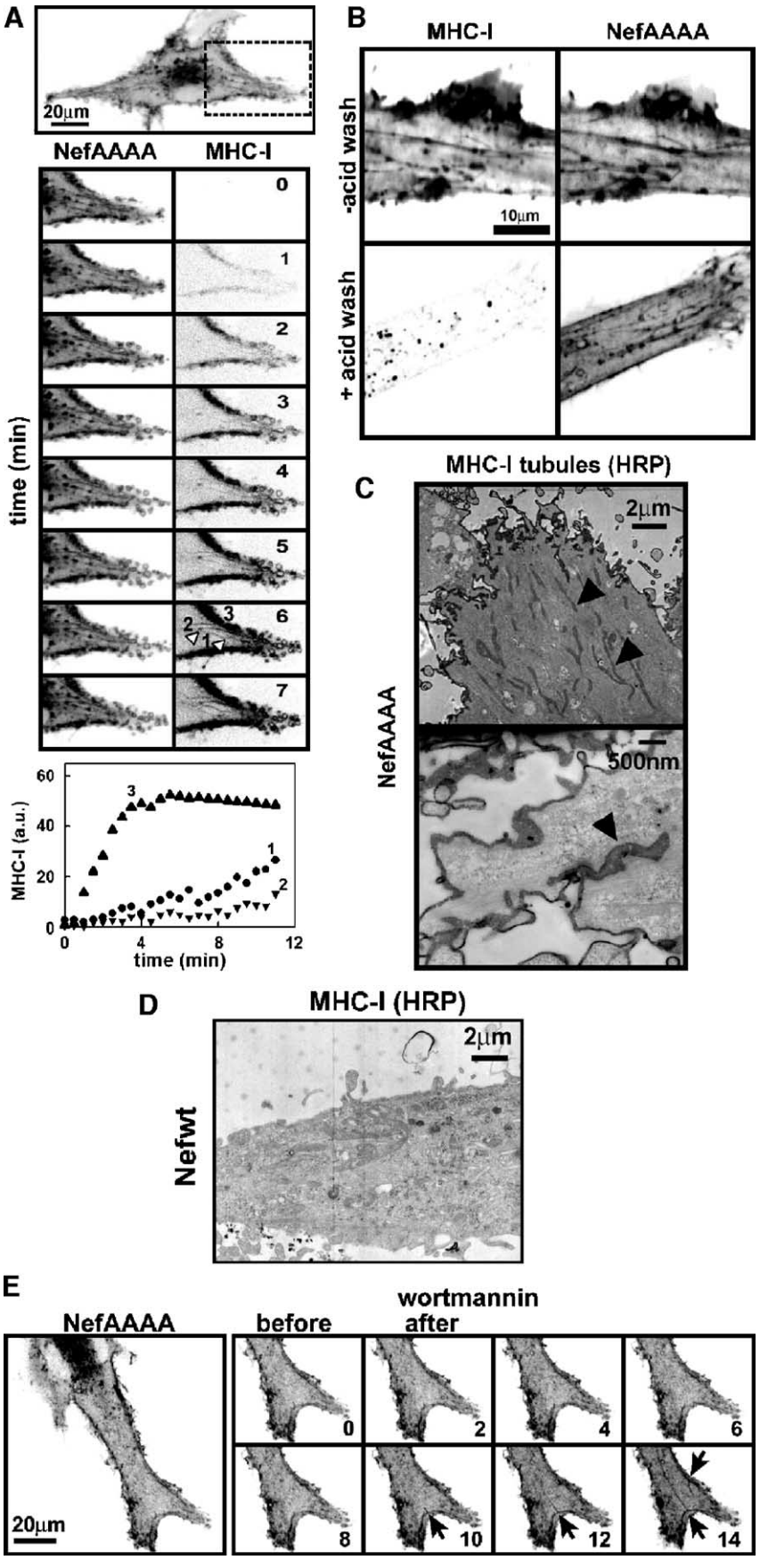
A
20μm
NefAAAA
MHC-I
time (min)
0
1
2
3
4
5
6
7
MHC-I (a.u.)
time (min)
B
MHC-I
NefAAAA
-acid wash
+ acid wash
10μm
C
MHC-I tubules (HRP)
NefAAAA
2μm
500nm
D
MHC-I (HRP)
Nefwt
2μm
E
NefAAAA
before
wortmannin
after
20μm
0
2
4
6
8
10
12
14

against MHC-I was added after fixation, this result clearly shows that the tubules were open and accessible to the extracellular media. Occasionally we observed direct continuity between the plasma membrane and deep invaginations of tubular shape labeled with DAB (Fig. 3C, arrow). As a control, we also observed cells not expressing NefAAAA and found DAB labeling restricted to the plasma membrane (not shown).

Finally, we made use of the fact that inhibition of PI3-K activity in cells expressing NefAAAA-EGFP increases the number of cells exhibiting tubules as an attempt to identify the possible site of formation of these structures. For this purpose, we observed cells expressing NefAAAA-EGFP using live-cell imaging after the addition of 0.5 μM wortmannin. We found many instances of NefAAAA-EGFP tubules emanating from the plasma membrane and extending towards the cell interior (Fig. 3D). Taken together, the results just described indicate that the NefAAAA tubules are unusual membrane structures that project deep into the cell, which often remain accessible to the extracellular milieu.

The long and stable tubular network enhanced by overexpression of NefAAAA or PI-3K inhibition segregates out from this compartment some markers of the plasma membrane such us Tf receptors. This latter was also observed in the relatively short, dynamic tubules regulated by Arf6, EHD1, and Rab22 [16,25]. The tubular network we have described here, however, is distinct from the Arf6-regulated tubules involved in MHC-I recycling from endosomes to the plasma membrane. Apart from their morphological and dynamic differences, and their differential sensitivity to wortmannin, the NefAAAA-enhanced tubules are partly opened to the cell surface and allow the internalization of MHC-I into the tubules, which is not observed in the Arf6-regulated recycling tubules [16]. Expression of NefAAAA or treatment with wortmannin does not increase the endocytic rate of MHC-I otherwise seen by expression of wild type Nef [17]. Thus, the MHC-I-containing tubules generated by NefAAAA expression do not seem to be major contributors to MHC-I transport into endosomes or for downmodulation of MHC-I mediated by wild type Nef. Nonetheless, to accurately measure the additional contribution in MHC-I internalization by this tubular pathway, we should achieve a condition were at least 80% of the cells express the tubular phenotype.

At present, it is not clear why the tubules reach the perinuclear endosomes. Regardless of the mechanism, this could be a way to ensure proximity between regions of the plasma membrane and deeper portions of the endosomal compartment to facilitate directed traffic between them (Fig. 4). This hypothesis is supported by the traffic of NefAAAA molecules from endosomes to the tubules (Fig. 2B). Additional studies will be necessary to clarify the role of this tubular network in MHC-I internalization and recycling.

Experimental procedures

Reagents and cells

Chemicals, antibodies, cells, plasmids, viral preparation, transfection, and transduction protocols were as previously described [17]. The EGFP-tagged HLA-A2 [28] construct was kindly provided by Dr. Hidde Ploegh, Harvard Medical School.

Sample handling and image acquisition and analysis

For fluorescence or electron microscopy experiments, U373mg astrocytoma cells were seeded at approximately 40–50% confluency on 18- or 25-mm glass or plastic coverslips 24 h before transfection or transduction. Cells were transfected with plasmids or transduced with several retroviral constructs, followed by imaging 48–72 h after. Live-cell imaging experiments were carried out as described [11]. Analysis of images was performed using Slidebook (Intelligent Imaging Innovations, Denver, CO) and Image J (v1.29, NIH, USA).

Real-time imaging of MHC-I internalization in NefAAAA-transduced cells

U373mg cells grown on 25-mm coverslips were washed with sterile PBS^+ and then transferred to an open perfusion

Fig. 3. MHC-I molecules internalize into the tubular network. (A) U373mg astrocytoma cells expressing NefAAAA-EGFP and exhibiting tubules were selected for imaging. The cells were incubated with Alexa594-labeled antibodies specific for the ecto domain of MHC-I and imaged as a function of time. Images of selected time points (min) of a region of the cell (stippled box) are shown. The plot corresponds to the appearance of fluorescent signal at the plasma membrane (3) and at two positions along the selected tubule (arrowheads), one close (1) and the other far (2) from the cell surface. Data are representative of 4 independent real-time antibody uptake experiments. (B) Cells were allowed to internalize the Alexa594-labeled MHC-I antibodies for 30 min at 37°C and washed four times within 1 min with a buffer of neutral pH (PBS, pH 7.4) or an acidic pH (50 mM glycine, 150 mM NaCl, 1 mM $MgCl_2$, 0.1 mM $CaCl_2$, pH 2.5). Cells were then fixed and imaged. Data are representative of at least 30 cells observed in 2 independent experiments. (C) Electron microscopy of cells expressing NefAAAA were incubated with the antibody specific for MHC-I for 30 min at 37°C, followed by fixation and processing for HRP/DAB staining at room temperature. The images show two examples illustrating the presence of DAB on the plasma membrane and inside tubules (top, arrowheads) or in deep invaginations emanating from the cell surface (bottom, arrowheads). Data are representative of 2 independent transductions. (D) Control for the electron microscopy experiment described in panel (C). The cell expresses Nefwt and lacks the expanded tubular network. The electron microscopy image shows absence of HRP staining at the plasma membrane and tubules (compare to Fig. 3C), demonstrating the specificity of the HRP-DAB staining for the recognition of MHC-I at the plasma membrane and in the tubular structures shown in panel (C). (E) Time-lapse series from a cell expressing NefAAAA-EGFP before and after addition of 1 μM wortmannin. The time-series highlights the appearance of tubules extending from the plasma membrane upon addition of wortmannin. Data are representative of 2 independent experiments.

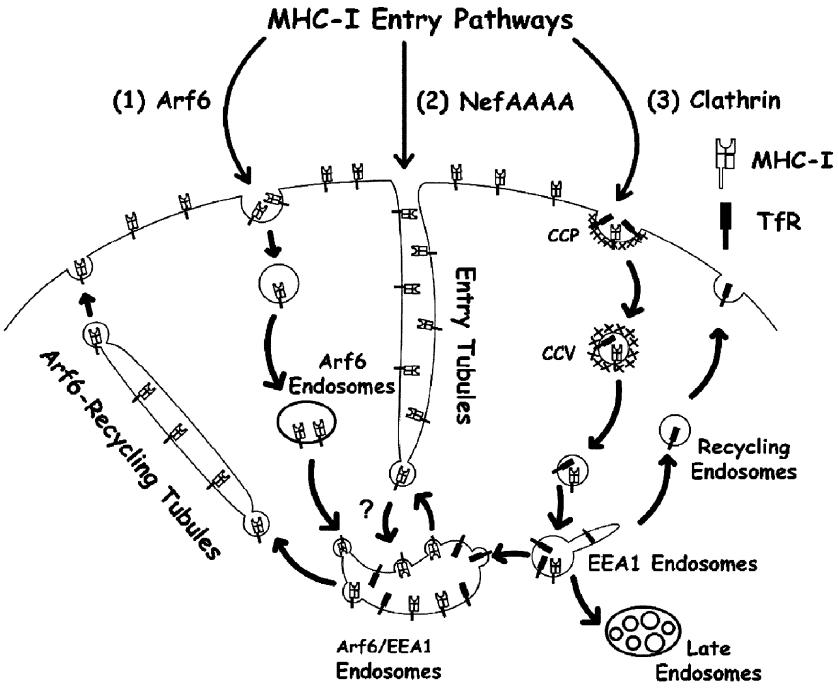

Fig. 4. Model for the intracellular traffic of MHC-I. The model illustrates multiple trafficking routes used by MHC-I molecules to move between the plasma membrane and the endosomal compartment.

chamber set at 37°C containing HMEMB medium. The time-lapse acquisition was started immediately after the addition of media containing the A594-labeled antibodies specific for the ecto-domain of MHC-I.

Photobleaching and photoactivation of NefAAAA

U373mg cells transduced with NefAAAA fused either to EGFP or to PA-GFP for 72 h were set for live cell imaging as described before. Photobleaching and photoconversion experiments were performed with a wavelength-tunable near-diffraction limited collimated laser beam (Photonics Instruments Inc., St. Charles, IL) generated by a nitrogen pulse laser (VSL-337ND-S, Laser Science Inc., Franklin, MA). The wavelength of the laser beam was tuned with a coumarine-based dye or with LD 423 (Photonics Instruments Inc., St. Charles, IL), with maximal emission at 490 nm or 422 nm, to specifically photobleach or photoconvert NefAAAA-EGFP or NefAAAA-PA-GFP, respectively. The laser, under computer control (Slidebook), was scanned on defined rectangular areas of selected cells showing a tubular phenotype due to NefAAAA expression. Photobleaching and photoconversion was achieved with minimal intensities and with exposures of less than 5 s to minimize photobleaching and phototoxic effects. Images on the EGFP channel were acquired immediately after photoconversion. NefAAAA diffusion coefficient was determined according to the equation: $D = 3r^2\gamma / 4t_{1/2}$ where r is the half-width of the bleach line, $t_{1/2}$ is the half-life of the recovery, and γ is a correction factor (0.6–0.9) for bleach depth [29].

Electron microscopy

NefAAAA transduced U373mg astrocytoma cells grown on plastic coverslips were incubated with mouse anti-MHC-I antibodies for 1–2 h at 37°C and then washed and fixed with 3% PFA. After quenching the samples with blocking buffer (Molecular Probes, Eugene, OR) to prevent endogenous peroxidase activity, cells were incubated with rabbit HRP-tagged anti-mouse antibodies (Molecular Probes, Eugene, OR) for 1 h at room temperature. The samples were then washed and incubated for 3 min at room temperature with diaminobenzidine/H_2O_2 followed by extensive washing steps (Molecular Probes, Eugene, OR). Cells were fixed with 2.5% glutaraldehyde/2% PFA in 0.1 M cacodylate buffer (pH 7.4) for 2 h at room temperature and processed for thin-section electron microscopy by epon resin embedding including osmium contrast enhancement. The images were acquired with a JEOL-100× microscope.

Acknowledgments

We thank Drs. Michel Franco, Mia Horowitz, Julie G. Donaldson, Jennifer Lippincott-Schwartz, Dan R. Littman, Hidde Ploegh, Victor Shu, Timothy A. Springer, Junichi Takagi, Domenico Tortorella, Roger Y. Tsien, and Rick van Etten for reagents. We also thank Dr. Lew Cantley for helpful advice concerning the PI3-K experiments, and Drs. Marcelo Ehrlich, Eric Macia, and Guillermo Romero for helpful discussions. The financial support to J.E.L. from the Danish Medical Research Council, the Danish AIDS

Foundation, and the Leo Nielsen and Karen Margarethe Nielsen Foundation is gratefully acknowledged.

Appendix A. Supplementary data

Supplementary data associated with this article can be found, in the online version, at doi:10.1016/j.yexcr.2005.01.021.

References

[1] K. Hirschberg, C.M. Miller, J. Ellenberg, J.F. Presley, E.D. Siggia, R.D. Phair, J. Lippincott-Schwartz, Kinetic analysis of secretory protein traffic and characterization of golgi to plasma membrane transport intermediates in living cells, J. Cell Biol. 143 (1998) 1485–1503.

[2] B.J. Nichols, A.K. Kenworthy, R.S. Polishchuk, R. Lodge, T.H. Roberts, K. Hirschberg, R.D. Phair, J. Lippincott-Schwartz, Rapid cycling of lipid raft markers between the cell surface and Golgi complex, J. Cell Biol. 153 (2001) 529–541.

[3] C. Yeaman, M.I. Ayala, J.R. Wright, F. Bard, C. Bossard, A. Ang, Y. Maeda, T. Seufferlein, I. Mellman, W.J. Nelson, V. Malhotra, Protein kinase D regulates basolateral membrane protein exit from trans-Golgi network, Nat. Cell Biol. 6 (2004) 106–112.

[4] P.J. Weidman, Anterograde transport through the Golgi complex: do Golgi tubules hold the key? Trends Cell Biol. 5 (1995) 302–305.

[5] R. Polishchuk, A. Di Pentima, J. Lippincott-Schwartz, Delivery of raft-associated, GPI-anchored proteins to the apical surface of polarized MDCK cells by a transcytotic pathway, Nat. Cell Biol. 6 (2004) 297–307.

[6] M. Boes, J. Cerny, R. Massol, M. Op den Brouw, T. Kirchhausen, J. Chen, H.L. Ploegh, T-cell engagement of dendritic cells rapidly rearranges MHC class II transport, Nature 418 (2002) 983–988.

[7] J. Tooze, M. Hollinshead, Tubular early endosomal networks in AtT20 and other cells, J. Cell Biol. 115 (1991) 635–653.

[8] S.J. Royle, L. Lagnado, Endocytosis at the synaptic terminal, J. Physiol. 553 (2003) 345–355.

[9] E.M. Danielsen, G.H. Hansen, Lipid rafts in epithelial brush borders: atypical membrane microdomains with specialized functions, Biochim. Biophys. Acta 1617 (2003) 1–9.

[10] G.H. Hansen, J. Pedersen, L.L. Niels-Christiansen, L. Immerdal, E.M. Danielsen, Deep-apical tubules: dynamic lipid-raft microdomains in the brush-border region of enterocytes, Biochem. J. 373 (2003) 125–132.

[11] R.H. Massol, J.E. Larsen, Y. Fujinaga, W.I. Lencer, T. Kirchhausen, Cholera toxin toxicity does not require functional Arf6- and dynamin-dependent endocytic pathways, Mol. Biol. Cell (2004) 3631–3641.

[12] M.E. Greenberg, A.J. Iafrate, J. Skowronski, The SH3 domain-binding surface and an acidic motif in HIV-1 Nef regulate trafficking of class I MHC complexes, EMBO J. 17 (1998) 2777–2789.

[13] F.D. Brown, A.L. Rozelle, H.L. Yin, T. Balla, J.G. Donaldson, Phosphatidylinositol 4,5-bisphosphate and Arf6-regulated membrane traffic, J. Cell Biol. 154 (2001) 1007–1017.

[14] S. Caplan, N. Naslavsky, L.M. Hartnell, R. Lodge, R.S. Polishchuk, J.G. Donaldson, J.S. Bonifacino, A tubular EHD1-containing compartment involved in the recycling of major histocompatibility complex class I molecules to the plasma membrane, EMBO J. 21 (2002) 2557–2567.

[15] N. Naslavsky, M. Boehm, P.S. Backlund Jr., S. Caplan, Rabenosyn-5 and EHD1 interact and sequentially regulate protein recycling to the plasma membrane, Mol. Biol. Cell 15 (2004) 2410–2422.

[16] R. Weigert, A.C. Yeung, J. Li, J.G. Donaldson, Rab22a regulates the recycling of membrane proteins internalized independently of clathrin, Mol. Biol. Cell (2004) 3758–3770.

[17] J.E. Larsen, R.H. Massol, T.J. Nieland, T. Kirchhausen, HIV Nef-mediated major histocompatibility complex class I down-modulation is independent of Arf6 activity, Mol. Biol. Cell 15 (2004) 323–331.

[18] H. Radhakrishna, J.G. Donaldson, ADP-ribosylation factor 6 regulates a novel plasma membrane recycling pathway, J. Cell Biol. 139 (1997) 49–61.

[19] K. Venkateswarlu, P.J. Cullen, Signalling via ADP-ribosylation factor 6 lies downstream of phosphatidylinositide 3-kinase, Biochem. J. 345 (Pt. 3) (2000) 719–724.

[20] K. Venkateswarlu, P.B. Oatey, J.M. Tavare, P.J. Cullen, Insulin-dependent translocation of ARNO to the plasma membrane of adipocytes requires phosphatidylinositol 3-kinase, Curr. Biol. 8 (1998) 463–466.

[21] S. Frank, S. Upender, S.H. Hansen, J.E. Casanova, ARNO is a guanine nucleotide exchange factor for ADP-ribosylation factor 6, J. Biol. Chem. 273 (1998) 23–27.

[22] D.J. Spiro, W. Boll, T. Kirchhausen, M. Wessling-Resnick, Wortmannin alters the transferrin receptor endocytic pathway in vivo and in vitro, Mol. Biol. Cell 7 (1996) 355–667.

[23] H. Shpetner, M. Joly, D. Hartley, S. Corvera, Potential sites of PI-3 kinase function in the endocytic pathway revealed by the PI-3 kinase inhibitor, wortmannin, J. Cell Biol. 132 (1996) 595–605.

[24] P.R. Shepherd, M.A. Soos, K. Siddle, Inhibitors of phosphoinositide 3-kinase block exocytosis but not endocytosis of transferrin receptors in 3T3-L1 adipocytes, Biochem. Biophys. Res. Commun. 211 (1995) 535–539.

[25] N. Naslavsky, R. Weigert, J.G. Donaldson, Convergence of non-clathrin- and clathrin-derived endosomes involves Arf6 inactivation and changes in phosphoinositides, Mol. Biol. Cell 14 (2003) 417–431.

[26] S. Nehls, E.L. Snapp, N.B. Cole, K.J. Zaal, A.K. Kenworthy, T.H. Roberts, J. Ellenberg, J.F. Presley, E. Siggia, J. Lippincott-Schwartz, Dynamics and retention of misfolded proteins in native ER membranes, Nat. Cell Biol. 2 (2000) 288–295.

[27] G.H. Patterson, J. Lippincott-Schwartz, A photoactivatable GFP for selective photolabeling of proteins and cells, Science 297 (2002) 1873–1877.

[28] S.A. Swann, M. Williams, C.M. Story, K.R. Bobbitt, R. Fleis, K.L. Collins, HIV-1 Nef blocks transport of MHC class I molecules to the cell surface via a PI 3-kinase-dependent pathway, Virology 282 (2001) 267–277.

[29] E.L. Feldman, D. Axelrod, M. Schwartz, A.M. Heacock, B.W. Agranoff, Studies on the localization of newly added membrane in growing neurites, J. Neurobiol. 12 (1981) 591–598.